Structural Investigation of High-Valent Manganese – Salen Complexes by UV/Vis, Raman, XANES, and EXAFS Spectroscopy

Martin P. Feth,*[a] Carsten Bolm,[b] Jens P. Hildebrand,[b] Manuela Köhler,[b] Oliver Beckmann,[b] Matthias Bauer,[a] Rivo Ramamonjisoa,[a] and Helmut Bertagnolli[a]

Abstract: XANES and EXAFS spectroscopic studies at the Mn – K- and Br – K-edge of reaction products of (*S*,*S*)-(+)-*N*,*N*′-bis(3,5-di-*tert*-butylsalicylidene)-1,2-cyclohexanediaminomanganese(III) chloride ([(salen)Mn^{III}Cl], **1**) and (*S*,*S*)-(+)-*N*,*N*′-bis(3,5-di-*tert*-butylsalicylidene)-1,2-cyclohexanediaminomanganese(III) bromide ([(salen)-Mn^{III}Br], **2**) with 4-phenylpyridine *N*-oxide (4-PPNO) and 3-chloroperoxybenzoic acid (MCPBA) are reported. The reaction of the Mn^{III} complexes with two equivalents of 4-PPNO leads to a hexacoordinated compound, in which the manganese atom is octahedrally coordinated by four oxygen/nitrogen atoms of the salen ligand at an average distance of ≈1.90 Å and two additional, axially bonded oxygen atoms of the 4-PPNO at 2.25 Å. The oxidation state of this complex was determined as ≈ +IV by a comparative study of Mn^{III} and Mn^{V} reference compounds. The green intermediate obtained in reactions of MCPBA and solutions of **1** or **2** in acetonitrile was investigated with XANES, EXAFS, UV/Vis, and Raman spectroscopy, and an increase of the coordination number of the manganese atoms from 4 to 5 and the complete abstraction of the halide was observed. A formal oxidation state of IV was deduced from the relative position of the pre-edge $1s \rightarrow 3d$ feature of the X-ray absorption spectrum of the complex. The broad UV/Vis band of this complex in acetonitrile with $\lambda_{max} =$ 648 nm was consistent with a radical cation structure, in which a MCPBA molecule was bound to the Mn^{IV} central atom. An oxomanganese(V) or a dimeric manganese(IV) species was not detected.

Keywords: manganese · N,O ligands · Raman spectroscopy · UV/Vis spectroscopy · XANES · X-ray absorption spectroscopy

Introduction

The asymmetric oxidation of alkenes is one of the most widely used methods for the synthesis of epoxides with high enantiomeric excesses. Several protocols have been described, which are based on the oxidation of the organic substrates with chiral metal catalysts.[1] Among the most established ones, the Jacobsen/Katsuki epoxidation of unfunctionalized alkenes with manganese(III) – salen complexes (H_2salen = bis(salicylidene)ethylenediamine) is known to proceed with a wide range of substrates affording products with very high enantioselectivies.[2] Despite its synthetic importance and the performance of numerous mechanistic investigations, surprisingly little is known about the exact path of the oxygen transfer. Furthermore, the precise nature of the catalytically active species is still under debate.[3] In almost all models it is proposed to be a [Mn^{V}=O(salen)] complex. Generally it is assumed that this oxomanganese complex is the reaction product of the manganese(III) – salen and the oxidant (e.g. 3-chloroperoxybenzoic acid (MCPBA)) and that it transfers its oxygen atom onto the olefin either in a stepwise radical process[4] or via a metallaoxetane.[5, 6] Alternatively, the Mn^{V}=O species can be formed by disproportionation of a μ-oxomanganese(IV) dimer.[7] The most striking evidence of the high-valent manganese species stems from electronspray mass spectrometry studies.[8] In view of this background we felt that UV/Vis, Raman, XANES, and EXAFS spectroscopy could also be useful tools in the search for high-valent manganese intermediates derived from manganese(III) – salen complexes and oxidants, such as MCPBA, in solution. Furthermore, we were interested in investigating the role of coligands, such as 4-phenylpyridine *N*-oxide (4-PPNO) or *N*-methylmorpholine *N*-oxide (NMO), which are known to increase the reaction rate and the enantioselectivity of the Jacobsen/Katsuki epoxidation.[4, 9] Herein, we present results of spectroscopic studies on two manganese(III) – salen complexes, (*S*,*S*)-(+)-

[a] M. P. Feth, M. Bauer, R. Ramamonjisoa, Prof. Dr. H. Bertagnolli
Universität Stuttgart, Institut für Physikalische Chemie
Pfaffenwaldring 55, 70569 Stuttgart (Germany)
Fax: (+49) 711-685-4443
E-mail: m.feth@ipc.uni-stuttgart.de

[b] Prof. Dr. C. Bolm, Dr. J. P. Hildebrand, M. Köhler, Dr. O. Beckmann
RWTH Aachen, Institut für Organische Chemie
Professor-Pirlet-Strasse 1, 52056 Aachen (Germany)
Fax: (+49) 241-809-23-91
E-mail: carsten.bolm@oc.rwth-aachen.de

Supporting information for this article is available on the WWW under http://www.chemeurj.org or from the author.

 © 2003 WILEY-VCH Verlag GmbH & Co. KGaA, Weinheim 0947-6539/03/0906-1348 $ 20.00+.50/0

N,*N*′-bis(3,5-di-*tert*-butylsalicylidene)-1,2-cyclohexanediaminomanganese(III) chloride ([(salen)Mn^{III}Cl], **1**) and (*S*,*S*)-(+)-*N*,*N*′-bis(3,5-di-*tert*-butylsalicylidene)-1,2-cyclohexanediaminomanganese(III) bromide ([(salen)Mn^{III}Br], **2**), and their reactions with 4-PPNO and MCPBA. As reference compound

The nitridomanganese(v) complex **3** was prepared as reference compound. Compounds **1**–**3** are illustrated in Scheme 1.

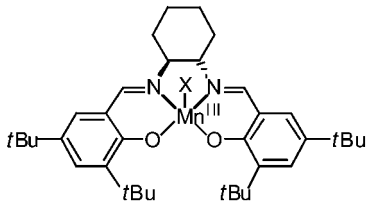

1: X = Cl, **2**: X = Br

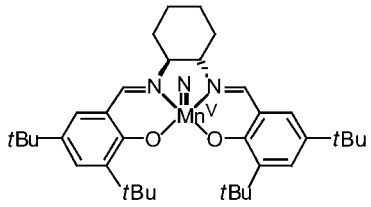

3

Scheme 1. Structural representations of complexes **1**–**3**.

XANES and EXAFS have proven to be powerful tools to elucidate the coordination sphere of catalytically active species in many cases.[10] We used X-ray absorption spectroscopy at the manganese and the bromine K-edge to investigate a possible ligand exchange of the manganese(III) complexes in the presence of 4-PPNO and the formation of high-valent species in solution after the addition of MCPBA as oxidant. First, comparative purposes, we present XANES and EXAFS measurements of the manganese(III)–salen complexes **1** and **2** as well as nitridomanganese(v) complex **3** [(salen)Mn^{V}N][11] in the solid state. The latter complex was regarded as an excellent reference compound for the detection of a possible [(salen)Mn^{V}=O]$^{+}$ intermediate resulting from the reaction of the Mn^{III} complexes with MCPBA, as the local structure around the metal center atoms of both [(salen)Mn^{V}=O]$^{+}$ and [(salen)Mn^{V}≡N], and therefore their XANES spectra and EXAFS functions, were expected to be similar. The interpretation of the XANES spectra will be focussed on the so-called pre-edge peaks (short: pre-peaks), which are related to dipole electron excitations from inner shells to unfilled bound states, for example 1s → 3d. These pre-peaks are very sensitive to geometrical changes in the first coordination shell of the absorbing atom. They can therefore be used as fingerprints for the presence of a certain coordination geometry.[12, 13] To obtain additional structural information UV/Vis, Raman, and IR studies were performed.

Results and Discussion

Electronic spectra: The absorption spectra of the orange-brown solutions of **1** and **2** in CH_2Cl_2 (Figure 1) show two poorly resolved bands at 439 and 493 nm. They are in good

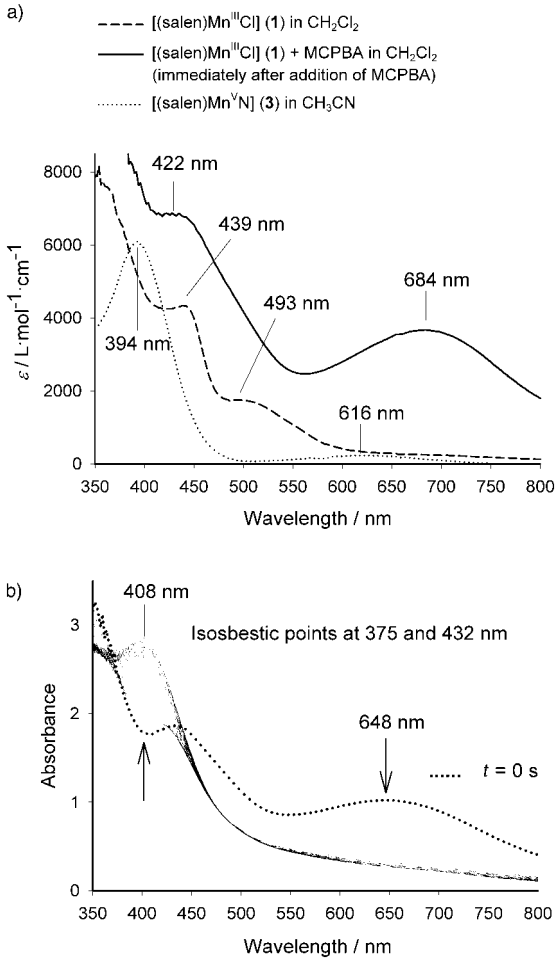

Figure 1. a) UV/Vis spectra of **1**, **1** + MCPBA, and **3** in CH_2Cl_2. b) UV/Vis spectra of **1** + MCPBA in CH_3CN in dependence of time (every 10 s).

agreement with that of *N*,*N*′-di(3-*tert*-butyl-5-methylsalicylidene)cyclohexanediaminemanganese(III) chloride in dichloromethane.[11] The UV/Vis spectrum of the light green solution of **3** in CH_2Cl_2 shows a strong band at 394 nm (Soret band) and a broad, weak band with $\lambda_{max} = 616$ nm ($\varepsilon_{max} \approx 230\ L\,mol^{-1}\,cm^{-1}$). When MCPBA is added in a 20-fold excess to a solution of **1**/**2** (0.3 mM) in dichloromethane, toluene, or acetonitrile, the color of the mixture immediately changes from orange-brown into dark green. This behavior was also observed by Adam et al., who oxidized **1** in CH_2Cl_2 with PhIO or NaOCl,[3a] and by Bortolini et al., who treated [(TMP)Mn^{III}Cl] with aqueous sodium hypochlorite solution to study high-valent manganese–porphyrin complexes.[14, 15] The spectrum of a solution of **1** after the addition of MCPBA in CH_2Cl_2 is also shown in Figure 1a. Compared with the unoxidized complex **1**, the spectrum of the resulting complex shows a new broad band with $\lambda_{max} = 684$ nm. In acetonitrile (Figure 1b) it is shifted to $\lambda_{max} = 648$ nm ($\varepsilon_{max} \approx$

 © 2003 WILEY-VCH Verlag GmbH & Co. KGaA, Weinheim 0947-6539/03/0906-1349 $ 20.00+.50/0

4400 $L\,mol^{-1}\,cm^{-1}$). However, as can be seen from the color change from green back to brown, the new species, which is formed when MCPBA is added, is not very stable at room temperature. This change is revealed by time-dependent UV/Vis spectra of **1** in CH_3CN after addition of MCPBA (Figure 1b). The absorbance of the solution at 648 nm decreases with time, and a new band at 408 nm is formed. Furthermore, from the two isosbestic points at 375 and 432 nm it can be concluded that only two species exist: the short-lived green intermediate and the brown reaction product. A kinetic analysis of the data indicates a first-order rate with respect to the intermediate species in acetonitrile with a rate constant of $k_1 = 6.20 \times 10^{-3}\,s^{-1}$ ($\tau_{1/2} = 112$ s). In toluene and in dichloromethane, rate constants of $k_1 = 2.44 \times 10^{-3}\,s^{-1}$ ($\tau_{1/2} = 284$ s) and $3.4 \times 10^{-2}\,s^{-1}$ ($\tau_{1/2} = 21$ s), respectively, were observed, revealing that in the latter solvent the reaction was much faster than in acetonitrile and toluene.

The formation of the intermediate was also observed when 4-PPNO was present as co-ligand in equal molar ratio to **1** or **2** to give **4** and **5**, respectively. Srinisvasan et al. found a new broad band with $\lambda_{max} = 530$ nm in the UV/Vis spectrum of a solution of a cationic *N,N′*-ethylenebis(salicylideneaminato)-manganese(III) complex in acetonitrile after oxidation with iodosylbenzene.[16] The authors interpreted this phenomenon with the formation of a thermally quite labile μ-oxomanganese(IV) dimer. Furthermore, they performed a kinetic analysis of the decay behavior of this intermediate in acetonitrile (monitored by the absorbance change at 680 nm). They found a first-order rate constant of $k_1 = 2.89 \times 10^{-3}\,s^{-1}$ ($\tau_{1/2} = 240$ s) at 25 °C, which is in good agreement with the results reported here. A broad band with $\lambda_{max} \approx 640$ nm ($\varepsilon_{max} \approx 6200\,L\,cm^{-1}\,mol^{-1}$) was also observed in a solution of $[(TPP)Mn^{IV}(OCH_3)_2]$ in dichloromethane,[15, 17] which was synthesized by oxidation of $[(TPP)Mn^{III}(OAc)]$ in methanol with iodosylbenzene. Groves et al., who investigated oxomanganese(V) porphyrin complexes by rapid-mixing stopped-flow spectrophotometry, related absorptions of oxidized Mn^{III} complexes near 700 nm to the presence of Mn^{IV} cation radicals.[18] Baldwin et al. found a band at 638 nm in an acetonitile solution of $[\{Mn^{IV}(salpn)\}_2(\mu\text{-}O,\mu\text{-}O{-}CH_3)](CF_3SO_3)$, which was treated with triflic acid.[15, 19] This band rapidly bleached to yellow-brown ($\lambda_{max} = 370$ nm). They assigned this band to the blue-shifted phenolate-to-Mn-transfer band (from the salpn ligand) of a protonated dimeric Mn^{IV} complex. In the nonprotonated form the transfer band was observed at 528 nm. As in our system, the green color can also be seen when $K_2S_2O_8$ is used as oxidant, a protonated transfer band of a dimeric Mn^{IV} complex is not very likely for our green product. The new band at 408 nm in the acetonitrile solution of the reaction product of **1** and **2**, after the decay of the short-lived green intermediate, is in good agreement with a Soret Band at 425 nm, found by Bortolini et al. from the brown product of the oxidation of $[(TMP)Mn^{III}Cl]$ with aqueous NaOCl solution.[14]

Raman and IR spectra: The Raman and IR spectra of the Mn^{III} complexes **1** and **2** are almost identical (Figure 2a). In the Raman spectra of both compounds a double peak at 557 and 569 cm^{-1} can be detected, which is absent in the spectrum of the pure salen. This double peak can also be seen in the IR spectra at 545 and 569 cm^{-1}. Typical metal–nitrogen stretching vibrations occur in Mn^{III} complexes between 230 (pyridine complexes) and 610 cm^{-1} (ethylendiamine complexes).[20] In Mn^{III}–porphyrin complexes, these values are typical for $Mn^{III}{-}O_{Lig}/N_{Lig}$ stretching vibrations.[17] Thus the double peak can be assigned to $Mn{-}O_{Salen}/N_{Salen}$ stretching vibrations. Since typical metal–chlorine stretching vibrations of Mn^{III} complexes are visible between 300–400 cm^{-1},[20] Raman spectroscopy was used for the detection of this vibration. The very weak signal at 381 cm^{-1} of the Raman spectrum, visible in compound **1** but absent in compound **2**, can be assigned to the Mn–Cl vibration. The Mn–Br vibration, which was expected to occur at a lower wave number, was not detected. Most likely, this weak signal was superposed by stronger Raman signals in this spectral range. In the Raman spectra of compounds **4** and **5**, as well as those of **6** and **7** (isolated solid products of **1** and **2**, respectively, upon addition

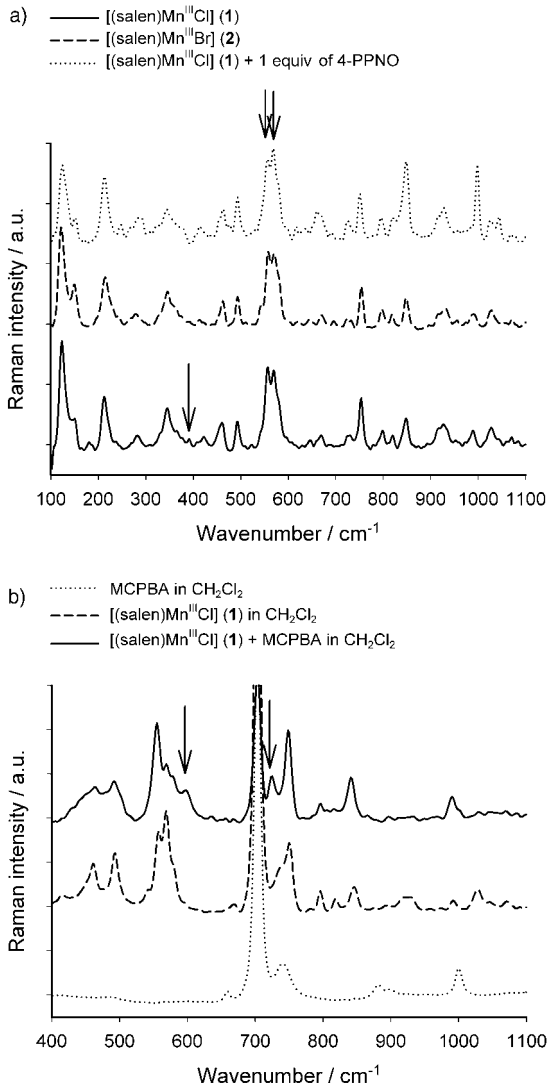

Figure 2. a) Raman spectra of solid **1**, **2**, and the isolated solid product of **1** + 1 equiv of 4-PPNO (**4**). b) Raman spectra of MCPBA in CH_2Cl_2, **1** in CH_2Cl_2 and **1** in CH_2Cl_2 oxidized with MCPBA.

© 2003 WILEY-VCH Verlag GmbH & Co. KGaA, Weinheim
0947-6539/03/0906-1350 $ 20.00+.50/0 *Chem. Eur. J.* **2003**, *9*, No. 6

of one or two equivalents of 4-PPNO), the intensity of the Raman peak at 569 is larger than that at 545 cm^{-1}. As 4-PPNO has no Raman peaks in this range, this might be regarded as evidence for changes in the first coordination sphere of the manganese central atom. Furthermore, the weak peak at 381 cm^{-1} is not present in compound **4**. Thus, we conclude that chloride was abstracted from the complex. In the Raman spectra of **4** and **5** the presence of 4-PPNO can easily be detected by comparison of the spectra with that of pure 4-PPNO. No indication for an oxygen transfer from 4-PPNO to the Mn^{III} complexes **1** and **2**, like typical Mn^{IV}=O vibrations of Mn^{IV} complexes at ≈800 cm^{-1},[21] were found. The presence of a coordinated 4-PPNO molecule with a weak Mn–O single bond can neither be excluded nor proven by the Raman spectra, as no significant new signals were detected in the range 400 – 600 cm^{-1}. Kochi and co-workers found 4-PPNO coordinated axially to a [(salen)Cr^{V}=O] complex at a distance of 2.18 Å.[22] This means that 4-PPNO is at best weakly bonded to the manganese central atom and, therefore, the Raman signal of the Mn–$O_{4\text{-PPNO}}$ vibration remains undetectable. In compound **3** the typical Mn^{V}≡N stretching frequency of a nitridomanganese(v) complex[23, 24] was observed at 1047 cm^{-1} in the Raman spectrum and at 1049 cm^{-1} in the infrared spectrum (figure not shown). The Mn–O/N stretching frequencies of the salen-ligand with the manganese central atom in **3** were found at 573 cm^{-1} as a single peak in the Raman spectrum and as a double peak at 542 and 565 cm^{-1} in the IR spectrum.

Raman investigations were also performed on the oxidized systems (Figure 2b). A concentrated solution of complex **1** in dichloromethane was oxidized with an equimolar amount of MCPBA. In this concentrated solution the green intermediate was found to be more stable than in the diluted solutions used for UV/Vis spectroscopy. In the oxidized sample two new Raman signals were observed at 599 and 725 cm^{-1}. Signals between 900 – 1000 cm^{-1}, which are typical of Mn^{V}=O vibrations in oxomanganese(v) complexes[22], or at ≈800 cm^{-1}, which indicate the presence of dimeric μ-oxo-bridged manganese(iv) complexes[7, 21] or oxomanganese(iv) complexes,[21] were not found. For comparative purposes, a solution of complex **1**, which was oxidized with $K_2S_2O_8$, was measured. In this dark green solution the same two signals were detectable at 601 and 724 cm^{-1}. Bortolini et al. found in the IR spectra of dichloromethane solutions of oxidized (with aqueous NaOCl solution) [(TMP)Mn^{III}Cl] comparable signals at 605 and 710 cm^{-1}.[14] The signal at 605 cm^{-1} was shifted to 610 cm^{-1}, when aqueous NaOBr solution was used for the oxidation, and shifted to 583 cm^{-1}, when labeled $Na^{18}OBr$ was used. They assigned the signal at ≈600 cm^{-1} to a Mn–O single bond and concluded, that –OCl or –OBr was coordinated to the manganese central atom. The signal at 725 cm^{-1} in our, and at 710 cm^{-1} in Bortolini's, system can be attributed to a weak Mn^{IV}=O bond as reported by Groves and co-workers in resonance Raman (RR) and IR spectroscopic investigations on oxomanganese(iv) – porphyrin complexes.[25] They found signals in the spectral range of 711 – 757 cm^{-1}, depending on the *trans*-axial ligand of the complex. The two bands in our oxidized system might be a hint for the presence of two different Mn^{IV} species with single and double-bonded oxygen at the manganese central atom. However, no evidence for the presence of a Mn^{V} or a dimeric Mn^{IV} species was found.

XANES and EXAFS spectra: *Mn K-edge XANES spectra*: From the XANES (X-ray absorption near edge structure) region of an X-ray absorption spectrum, information about the coordination geometry of the first coordination shell around an absorbing atom can be obtained.[26] The X-ray absorption edge position indicates the charge of the absorbing atom. Since it is strongly affected by changes in the coordination geometry,[12] information about the oxidation state of the absorbing atom can also be misleading. In the XANES region, and also some electron Volts before the absorption edge, further absorptions can take place, caused by the transitions of electrons from inner shells (such as 1s) to unoccupied states (such as 3d).[12] Such features are called pre-peaks. The strength of such pre-peaks strongly depends on the coordination symmetry around the absorbing atom,[13] and it can therefore be used as an indicator for symmetry changes at the catalytic active center (for example the manganese central atom in the manganese salen complex) during chemical reactions. The energetic position of the pre-peak depends also on the oxidation state of the absorbing atom, but is not affected by multiple scattering. It therefore provides more reliable information than the edge position. XANES and pre-edge investigations are usually made as comparative studies. Compounds **1** and **2** were used as Mn^{III} reference samples. Compound **3** allowed monitoring of the oxidation state +v. The XANES spectra of **1**, **2**, and **3** at the Mn K-edge are shown in Figures 3 and 4. Table 1 summarizes the energetic positions (E_{PP}) and the energetic shift (δ), compared to compound **3**, of the pre-peak features in these compounds.

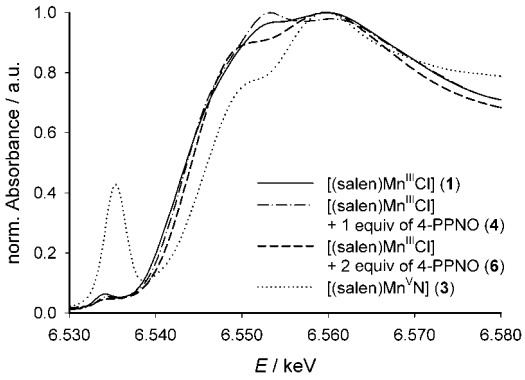

Figure 3. Comparison of the Mn K-edge XANES regions of solid [(salen)-Mn^{III}Cl] (**1**), the isolated solid product **4** of [(salen)Mn^{III}Cl] + 1 equiv of 4-PPNO, the isolated solid product **6** of [(salen)Mn^{III}Cl] + 2 equiv of 4-PPNO, and solid [(salen)Mn^{V}N] (**3**).

Since electric dipole transitions [1s → (A_1,E)] in high-valent manganese(iv/v) complexes are allowed for a ligand field with approximately C_{4v} symmetry, whereas in hexacoordinated complexes with D_{4h} or D_{2h} symmetry such transitions are classically forbidden,[14, 18] the manganese(v) reference compound **3** exhibited a very strong 1s → 3d pre-peak feature at 6535.3 eV, which was also described for [(TMP)Mn^{V})N].[14] Another reason for the amazing strength of the pre-peak

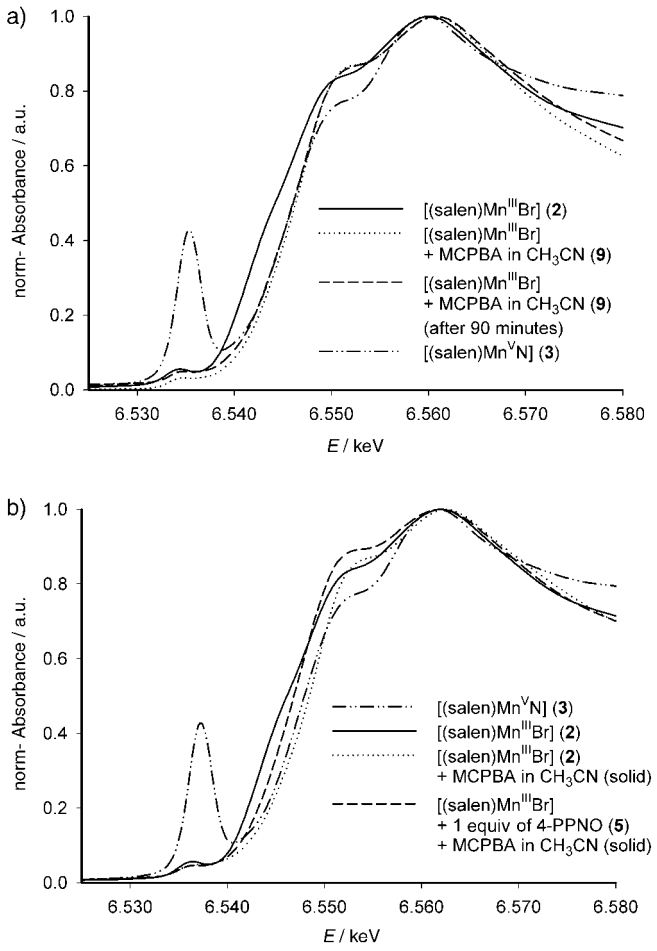

Figure 4. Comparison of the Mn K-edge XANES regions of the oxidized [(salen)Mn^{III}Br] (**2**) in acetonitrile. a) Solid [(salen)Mn^{III}Br] (**2**), **2** oxidized with MCPBA in acetonitrile after 0 min, **2** oxidized with MCPBA in acetonitrile after 90 min (dotted line), solid [(salen)Mn^{V}N] (**3**). b) Solid [(salen)Mn^{III}Br] (**2**), isolated solid product of **2** + MCPBA in acetonitrile, isolated solid product of **2** + 1 equiv of 4-PPNO + MCPBA in acetonitrile, solid [(salen)Mn^{V}N] (**3**).

Table 1. Positions (E_{PP}) and shifts of the pre-edge features (δ) in the investigated manganese complexes relative to the energy position of the pre-edge feature in compound **3**, determined from the Mn K-edge XANES spectra.

Compound	E_{PP} [eV]	$\delta = E_{PP} - E_{PP,3}$ [eV]
[(salen)Mn^{III}Cl] (**1**)	6534.1 ± 0.2	− 1.2
[(salen)Mn^{III}Br] (**2**)	6534.3 ± 0.2	− 1.0
1 + 2 equiv of 4-PPNO (**6**)	6534.8 ± 0.2	− 0.5
2 + 2 equiv of 4-PPNO (**7**)	6534.8 ± 0.2	− 0.5
1 + 1 equiv MCPBA in acetonitrile (**8**)	6534.7 ± 0.2	− 0.6
2 + 1 equiv MCPBA in acetonitrile (**9**)	6534.8 ± 0.2	− 0.5
2 + 1 equiv MCPBA in acetonitrile (**9**) (after 90 min)	6534.6 ± 0.2	− 0.7
isolated solid product of **2** oxidized with 1 equiv of MCPBA in acetonitrile	6534.6 ± 0.2	− 0.7
isolated solid product of **2** + 1 equiv of 4-PPNO oxidized with 1 equiv of MCPBA in acetonitrile	6534.6 ± 0.2	− 0.7
2 + 1 equiv 4-PPNO + 1 equiv MCPBA in acetonitrile (**11**)	6534.8 ± 0.2	− 0.5
[(salen)Mn^{V}N] (**3**)	6535.3 ± 0.2	0.0
[(TMP)Mn^{III}Br][14]		− 1.4
[(TMP)Mn^{IV}(OCl)][14]		− 0.6
[(TMP)Mn^{V}N][14]		0.0

could be due to the so-called "molecular-cage-size effect", described by Kutzler et al.[27] and Lytle and co-workers.[13] They found that the strength of the pre-peak transition depended on the size of the molecular-cage defined by the nearest neighbour atoms coordinating the X-ray absorbing center. A cage-size parameter R can be defined as an average bond distance of all nearest neighbours. The pre-peak intensity increases at a given geometry with decreasing cage-size parameter. Lytle and co-workers found this behavior in several vanadium compounds, for example in the five-coordinate, distorted tetragonal pyramidal compounds V_2O_5 ($R = 1.83$ Å), VOPBD[15] ($R = 1.90$ Å) and $VOSO_4 \cdot 3H_2O$ ($R = 1.95$ Å), where V_2O_5 had the highest and $VOSO_4 \cdot 3H_2O$ the lowest pre-peak intensity. Therefore a high-valent oxomanganese(v) complex with C_{4v} symmetry, postulated as the active catalytic species in the enantioselective epoxidation of olefins, should also be expected to show such a high pre-peak feature and therefore be easily detectable. The $1s \rightarrow 3d$ transition can be observed in the Mn^{III} complexes **1** and **2** as well; however, the pre-peak intensity is significantly smaller than in the Mn^{V} reference compound **3** and shifted towards lower energies (6534.1 eV in the case of **1** and 6534.3 eV in **2**). The energetic shifts δ compared to **3** are − 1.2 eV for complex **1** and − 1.0 eV for complex **2**. These values are in good agreement with those found by Bortolini et al. for manganese(III/V) porphyrin complexes.[14]

Figure 3 also shows the Mn K-edge XANES spectra of compounds **4** and **6**. The absorption edge, as well as the pre-peak position in **4** and **5**, are shifted towards higher energies. This is also observed in the corresponding compounds **6** and **7**. The pre-peak position shifts (δ) of **6** and **7** (Table 1) fit to the one reported for a Mn^{IV} complex by Bortolini et al.[14] Since differences in the edge position of **4** and **6** (**5** and **7**) can be detected, different structures in the reaction products of **1** (**2**) with one or two equivalents of 4-PPNO must be expected. In Figure 4a and 4b the XANES spectra of the oxidized systems are shown. The solution of **2** oxidized with 1 equivalent of MCPBA in acetonitrile (to give **9**) (Figure 4b) shows an absorption edge, which is shifted to higher energies compared with **2** and even with **3**. However, the pre-peak position has an intermediate value between the two extremes Mn^{III} and Mn^{V}, thus the manganese central atom is most probably in the valence state +IV. The pre-peak height of the solution of **9** is lower than the one for compound **3**, which shows that the formation of an oxomanganese(v) complex with C_{4v} symmetry is unlikely. This fits to the results reported by Bortolini et al.[14]

In the XANES spectra of the solution recorded 90 minutes after adding the oxidant (Figure 4a) no significant changes were observed. Actually the edge position has a slight shift to lower energies, which might indicate that some of the oxidized complex is reduced again to Mn^{III} or that another Mn^{IV} complex is formed. The same result was obtained, when complex **1** was oxidized with MCPBA in acetonitrile (to give **8**). From a solution of **2**, which was oxidized with two equivalents of MCPBA in acetonitrile (**9**), a dark green amorphous product was isolated after evaporation of the solvent. The XANES spectrum of this product is shown in Figure 4b. Again, no indication for an oxomanganese(v) complex was observed. The position of the pre-peak and the

 © 2003 WILEY-VCH Verlag GmbH & Co. KGaA, Weinheim 0947-6539/03/0906-1352 $ 20.00+.50/0 *Chem. Eur. J.* **2003**, *9*, No. 6

absorption edge showed that the green complex was quite stable under the conditions of the reaction (molar ratio oxidant/complex 1:1, high concentrated solution), as no shifts in the absorption edge/pre-peak compared with the solution of **9** were detected. At the end of the XANES and EXAFS study the investigated solutions still had a dark green color.

When a mixture of the isolated olive-brown solid product of complex **2** and one equivalent of 4-PPNO was oxidized with two equivalents of MCPBA in acetonitrile (to give **11**) the absorption edge and the pre-peak were significantly shifted to lower energies, compared with the solid product without 4-PPNO. Evidently, the oxidized complex shows a higher rate of decomposition in the presence of the co-ligand.

EXAFS analysis at the Mn K-edge and Br K-edge: The structural parameters determined by Mn K-edge and Br K-edge EXAFS on solid Mn^{III} (**1**, **2**) and Mn^{V} reference compounds are summarized in Table 2. The EXAFS function (Mn K-edge) of complex **1** (Figure 5a) was fitted with a three-shell model. The first coordination shell at ≈1.9 Å, visible as a strong peak in the Fourier-transformed (FT) EXAFS spectrum in Figure 5b, consists of nitrogen and oxygen backscatterers of the coordinated salen ligand. As oxygen and nitrogen atoms have almost the same amplitude and phase functions, and moreover, as known from XRD, the Mn–N and Mn–O distances of the coordinated salen ligand do not differ significantly, this shell was only fitted with oxygen backscatterers. The peak at ≈2.3 Å of the FT spectrum can be assigned to a chlorine backscatterer, the signal at 2.8 Å to further carbon backscatterers of the salen ligand. The determined coordination numbers and distances in compound **1** are in very good agreement with those found by single-crystal XRD studies.[11, 28] The same fitting procedure was performed with the EXAFS function of complex **2** (Mn K-edge). The structural parameters of the first N/O coordination shell of **1** and **2** are quite similar. The bromine backscatterer in **2** was found at 2.54 Å, which is in good agreement with a Mn–Br distance of 2.51 Å found in [(TMP)Mn^{III}Br].[14] This distance was verified by EXAFS measurements at the Br K-edge of complex **2**.

Table 2. Structural parameters of solid reference Mn^{III} and Mn^{V} complexes, determined from the Mn K-edge and Br K-edge EXAFS spectra.[a]

	A – Bs	r [Å]	N	σ [Å]	ΔE_0 [eV]	k-range [Å^{-1}] fit index
[(salen)Mn^{III}Cl] (**1**),	Mn–O/N	1.90 ± 0.02	4.2 ± 0.4	0.084 ± 0.008	20.5	3.30 – 15.00
solid-state EXAFS	Mn–Cl	2.39 ± 0.02	0.9 ± 0.2	0.081 ± 0.012		25.7
	Mn–C	2.89 ± 0.03	3.6 ± 1.1	0.055 ± 0.015		
[(salen)Mn^{III}Cl] (**1**) in	Mn–O/N	1.91 ± 0.02	3.8 ± 0.4	0.081 ± 0.008	19.7	3.03 – 11.00
acetonitrile,	Mn-Cl	2.37 ± 0.02	1.0 ± 0.2	0.100 ± 0.015		27.8
liquid-state EXAFS	Mn-C	2.89 ± 0.03	4.4 ± 1.1	0.077 ± 0.023		
[(salen)Mn^{III}Br] (**2**),	Mn–O/N	1.89 ± 0.02	4.1 ± 0.4	0.081 ± 0.008	19.0	3.09 – 15.00
solid-state EXAFS	Mn–Br	2.54 ± 0.03	0.9 ± 0.2	0.081 ± 0.012		26.1
	Mn–C	2.91 ± 0.03	5.0 ± 1.5	0.067 ± 0.020		
	Br–Mn	2.53 ± 0.03	0.9 ± 0.1	0.071 ± 0.007	19.2 32.3	3.65 – 12.30
[(salen)Mn^{V}N] (**3**),	Mn–N	1.51 ± 0.01	1.2 ± 0.4	0.059 ± 0.006	25.9	3.50 – 16.00
solid-state EXAFS	Mn–O/N	1.91 ± 0.02	3.8 ± 0.2	0.063 ± 0.006		23.7
	Mn–C	2.89 ± 0.03	3.7 ± 1.2	0.063 ± 0.017		
[(salen)Mn^{III}Cl] (**1**)	Mn–O/N	1.93	4			
single-crystal XRD[11]	Mn–Cl	2.39	1			
[(salen)Mn^{III}Cl] (**1**)	Mn–O/N	1.92	4			
single-crystal XRD[28]	Mn–Cl	2.36	1			
[(salen)Mn^{V}N][b]	Mn–N	1.54	1			
single-crystal XRD[24]	Mn–O/N	1.93	4			
[(saltmen)Mn^{V}N][c]	Mn–N	1.51	1			
single-crystal XRD[23a]						
[(TMP)Mn^{III}Br][d],						
	Mn–N	1.99	4			
	Mn–Br	2.51	1			
	Mn–C	3.02	? [g]			
Solid-state EXAFS[14]						
[(TMP)Mn^{V}N][d]	Mn–N	1.50	1			
solid-state EXAFS[14]	Mn–N	2.01	4			
[(dmOEP)Mn^{V}N][e]	Mn–N	1.51				
single crystal XRD[23b]						
[($DPPF_{20}$)Mn^{III}Cl][f]	Mn–N	2.00	4			
EXAFS[29]	Mn-Cl	2.37	1			
[($DPPF_{20}$)Mn^{III}Br][f]	Mn–N	2.00	4			
EXAFS[29]	Mn-Br	2.51	1			
[($DPPF_{20}$)Mn^{V}N][f]	Mn–N	1.51	1			
EXAFS[29]	Mn–N	2.01	4			

[a] Absorber (A) - backscatterer (Bs) distance r, coordination number N, Debye – Waller factor σ with their calculated deviation, shift of the energy threshold ΔE_0. [b] Salen: (*R*,*R*)-diphenyl-*tert*-butylmethylsalen [c] Saltmen: 2,3-diamino-2,3-dimethylbutane backbone in the salen ligand without *tert*-butyl groups [d] TMP: chloro-(5,10,15,20-*meso*-tetramesitylporphorin) [e] dmOEP: 5,15-dimethyl-2,3,7,8,12,13,17,18-octaethyl-5*H*,15*H*-porphorin. [f] $DPPF_{20}$: *meso*-5,10,15,20-tetrakispentafluorophenyl-2,3,7,8,12,13,17,18-octakisphenylporphorin. [g] Coordination number is not given in the reference.

In the manganese(v) reference compound **3** the short manganese – nitrogen separation of the nitrido group was found at 1.51 Å, visible as a shoulder at 1.5 Å in the FT-EXAFS spectrum at the Mn K-edge (Figure 5d). This value is in excellent agreement with those found for similar nitrido-manganese(v) complexes.[14, 23a, 14, 29] Table 3 summarizes the structural parameters of the reaction products of **1** and **2** with 4-PPNO (**4** and **5**, respectively). In both case, where one equivalent of 4-PPNO was added to **1** or **2**, a significant reduction of the halogen contribution in the EXAFS function and a decrease of the peak intensity of the halogen backscatterer in FT-EXAFS spectrum was observed. This is visualized in Figure 6a and 6b for system **5**.

The coordination number of the chlorine backscatterer decreases from 0.9 to 0.5 in the case of system **4**, and from 1.0

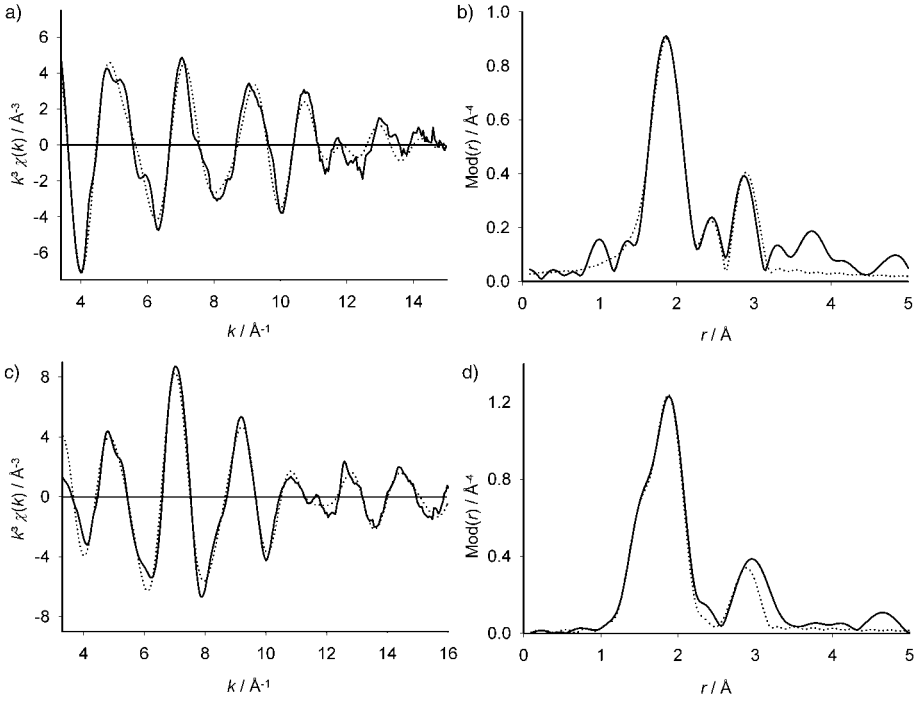

Figure 5. a,b) Experimental (solid line) and calculated (dotted line) $k^3\chi(k)$ functions (a) and their Fourier transforms (b) of solid [(salen)Mn^{III}Cl] (**1**) (Mn K-edge). c,d) Experimental (solid line) and calculated (dotted line) $k^3\chi(k)$ functions (c) and their Fourier transforms (d), of solid [(salen)Mn^{V}N] (**3**) (Mn K-edge).

Table 3. Structural parameters of the Mn^{III} complexes with addition of 4-PPNO determined from the Mn K-edge and Br K-edge EXAFS spectra.[a]

	A – Bs	r [Å]	N	σ [Å]	ΔE_0 [eV]	k-range [Å^{-1}] fit index
4: 1+1 equiv of 4-PPNO	Mn–O/N	1.91 ± 0.02	4.0 ± 0.4	0.081 ± 0.008	20.8	3.14 – 14.50
solid-state EXAFS	Mn–Cl	2.43 ± 0.02	0.5 ± 0.1	0.074 ± 0.011		30.9
	Mn–C	2.88 ± 0.03	3.8 ± 1.0	0.055 ± 0.015		
6: **1** + 2 equiv of 4-PPNO	Mn–O/N	1.90 ± 0.02	4.0 ± 0.4	0.087 ± 0.009	23.4	3.62 – 12.50
solid-state EXAFS	Mn–O	2.25 ± 0.02	1.8 ± 0.3	0.097 ± 0.015		25.2
	Mn–C	2.89 ± 0.03	3.7 ± 1.1	0.059 ± 0.017		
5: **2** + 1 equiv of 4-PPNO	Mn–O/N	1.89 ± 0.02	4.1 ± 0.4	0.081 ± 0.008	20.5	3.29 – 14.00
solid-state EXAFS	Mn–Br	2.56 ± 0.03	0.4 ± 0.2	0.081 ± 0.012		27.0
	Mn–C	2.91 ± 0.03	4.4 ± 1.3	0.059 ± 0.017		
	Br–Mn	2.53 ± 0.03	0.3 ± 0.1	0.071 ± 0.007	25.2 49.3	4.20 – 10.20
7: **2** + 2 equiv of 4-PPNO	Mn–O/N	1.89 ± 0.02	4.1 ± 0.4	0.084 ± 0.008	25.0	3.41 – 12.50
solid-state EXAFS	Mn–O	2.25 ± 0.02	1.6 ± 0.2	0.092 ± 0.012		25.7
	Mn–C	2.89 ± 0.03	3.8 ± 1.3	0.063 ± 0.021		
	Br–Mn	–	–	–	–	4.20 – 10.20

[a] Absorber (A) - backscatterer (Bs) distance r, coordination number N, Debye – Waller factor σ with their calculated deviation, shift of the energy threshold ΔE_0.

to 0.4 in the case of the bromine backscatterer in system **5**. Furthermore, a slight increase in the manganese halogen distance was found in both cases. In the reaction products **6** and **7**, where two equivalents of 4-PPNO were added to the managnese(III) complexes **1** and **2**, no halogen backscatterers contribute to the EXAFS function (Figures 6c and 6d).

For a better quantification of the halogen abstraction, systems **5** and **7** were investigated by EXAFS spectroscopy at the Br K-edge. The EXAFS functions together with their Fourier-transformations are shown in Figures 7a and 7b. The structural parameters prove the results of the EXAFS spectra at the Mn K-edge. The decrease of the manganese signal is clearly visible in the EXAFS function as well as in the FT spectra. In the Mn K-edge spectra of system **6** and **7** a new coordination shell of oxygen backscatterer was observed at 2.25 Å with a coordination number of ≈2. These oxygen atoms obviously belong to the 4-PPNO, thus the manganese central atom is hexacoordinate in these systems. The observation that two 4-PPNO molecules are axially coordinated to the manganese central atom, while the halogen atom is abstracted from the complex, is supported by the XANES investigations, from which a formal oxidation state of approximately +IV for the manganese atoms in systems **6** and **7** can be deduced. Furthermore, a recently published EPR study of Campbell et al. also supports our results.[30] From the comparison of the parallel mode EPR spectra of a dichloromethane solution of **1** with the dichloromethane solutions of **1** after addition of either 4-PPNO or NMO, they found indications for the axial coordination of two 4-PPNO (NMO) molecules to the manganese(III) complex, which leads to an octahedral geometry around the manganese center. The observed Mn–$O_{4\text{-PPNO}}$ distance of 2.25 Å also corresponds to a Cr–O_{PNO} distance of 2.18 Å found by Kochi and co-workers in a [(salen)Cr^{V}(oxo)(PNO)] complex.[22]

Table 4 shows the structural parameters, determined by Mn K-edge EXAFS, of the oxidized manganese systems. In all oxidized systems the halide of complexes **1** or **2** does not continue to contribute to the EXAFS function. Thus, it can be concluded that the addition of one equivalent of MCPBA leads to the complete abstraction of the halide from the complex. Figures 8a and 8b show a comparison of the EXAFS and FT-EXAFS spectra of the acetonitrile solutions of complex **2** with and without addition of 4-PPNO, respectively, after oxidation with one equivalent of MCPBA. Clearly visible in the FT spectra is the absence of the bromine backscatterer at ≈2.5 Å in both systems. In the oxidized

© 2003 WILEY-VCH Verlag GmbH & Co. KGaA, Weinheim
0947-6539/03/0906-1354 $ 20.00+.50/0 *Chem. Eur. J.* **2003**, *9*, No. 6

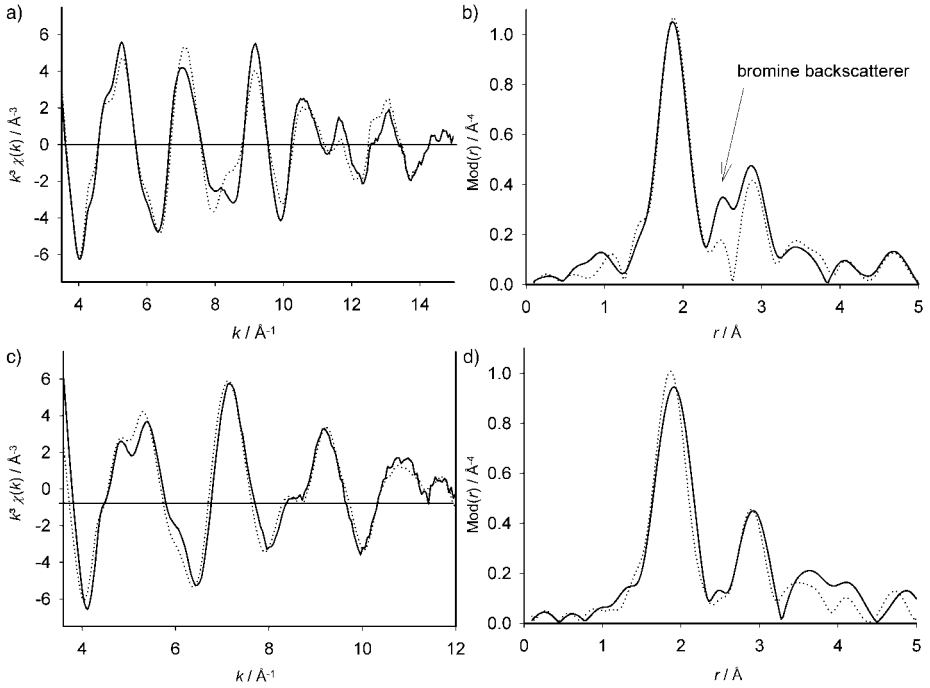

Figure 6. a,b) Comparison of the experimental $k^3\chi$(k) functions (a) and their Fourier transforms (b) of solid [(salen)Mn^{III}Br]] (**2**) (solid line), isolated solid product **5** of [(salen)Mn^{III}Br] + 1 equiv of 4-PPNO (dotted line) (Mn K-edge). c,d) Experimental (solid line) and calculated (dotted line) $k^3\chi(k)$ functions (c) and their Fourier transforms (d) of the isolated solid product **7** of [(salen)Mn^{III}Br] + 2 equiv of 4-PPNO (Mn K-edge).

system without the presence of 4-PPNO an increase in the coordination number of the first coordination shell from 4.1 to 4.8 was observed. The average length of the shell, however, shows no significant changes (1.90 Å in complex **1** and 1.89 Å in the oxidized sample). A short bonded backscatterer in the range of 1.5 – 1.6 Å, typical for a Mn^{V}=O bond, or manganese backscatterer at ≈2.7 – 2.8 Å, typical for dimeric Mn^{IV} species,[19] is not observed. Bortolini et al. reported in an [(TMP)Mn^{III}Cl] complex, oxidized with aqueous NaOCl solution, an additional oxygen backscatterer at 1.84 Å and related this oxygen atom to a coordinated OCl^-.[14]

This observation is in very good agreement with our result, as a calculated average distance of all five backscatterers (four of the salen ligand at 1.90 Å and one of the oxidant at 1.84 Å) would lead to a value of 1.89 Å, which is exactly the value determined by our EXAFS study. An oxygen backscatterer at 1.8 – 1.9 Å would also explain the Raman signal found at 599 cm^{-1} in the same system, which is typical for an Mn–O single bond. In the study of Bortolini et al. an additional backscatterer at 2.30 Å, assigned to a H_2O molecule, is discussed.[14] Their EXAFS results, however, did not prove the existence of this backscatterer, thus pentacoordination at the manganese central atom is most likely. A fivefold coordination is also more probable as the additional backscatterer has a relatively short distance (≈1.8 – 1.9 Å). In an octahedral coordination the distance is expected to be longer.[29] For example, for an octrahedral [$(DPPF_{20})Mn^{IV}(O_3)_2$] complex, two Mn–$O_{ozone}$ bond lengths of 2.09 Å have been found. This result, together with our XANES results, leads to the conclusion that a MCPBA molecule is coordinated with a Mn–O single bond to the manganese central atom, which is in the oxidation state +IV.

The EXAFS result of the oxidized solution of **2** in the presence of one equivalent of 4-PPNO does not reveal the presence of additional backscatterers. Neither bromide nor an oxygen atom of 4-PPNO is detectable. The absence of any additional backscatterer might be the result of a faster decomposition of the oxidized complex in this system, as mentioned in the XANES study.

Our EXAFS investigations on oxidized acetonitrile solutions of complex **1** (Table 4), are in complete agreement with the results found for the oxidized solutions of complex **2**.

To examine the stability of the oxidized complex **2**, the dark green, amorphous solid, which was isolated from the acetonitrile solution of **2** oxidized with two equivalents of MCPBA, was investigated by EXAFS. A comparison of the EXAFS

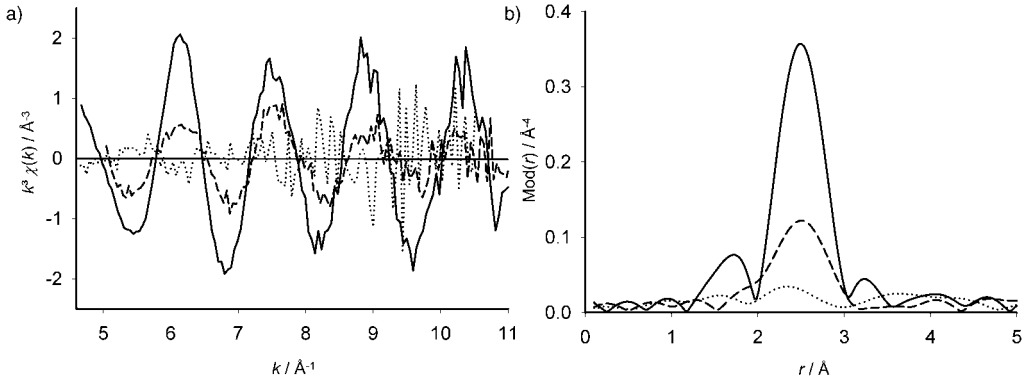

Figure 7. Comparison of the experimental $k^3\chi(k)$ functions (a) and their Fourier transforms (b) of solid [(salen)Mn^{III}Br]] (**1**) (solid line), isolated solid product **5** of [(salen)Mn^{III}Br] + 1 equiv of 4-PPNO (dashed line), and isolated solid product **7** of [(salen)Mn^{III}Br] + 2 equiv of 4-PPNO (dotted line) (Br K-edge).

 © 2003 WILEY-VCH Verlag GmbH & Co. KGaA, Weinheim 0947-6539/03/0906-1355 $ 20.00+.50/0

Table 4. Structural parameters of the oxidized Mn^{III} complexes with and without addition of 4-PPNO determined from the Mn K-edge EXAFS spectrum.[a]

	A – Bs	r [Å]	N	σ [Å]	ΔE_0 [eV]	k-range [$Å^{-1}$] fit index
1 + 1 equiv of MCPBA in acetonitrile (**8**), liquid-state EXAFS	Mn–O/N Mn–C	1.89 ± 0.02 2.87 ± 0.03	4.6 ± 0.5 4.0 ± 1.3	0.084 ± 0.008 0.089 ± 0.020	22.3	3.54 – 12.0 27.8
1 + 1 equiv of 4-PPNO + 1 equiv of MCPBA in acetonitrile (**10**), liquid-state EXAFS	Mn–O/N Mn-C	1.89 ± 0.02 2.88 ± 0.03	4.0 ± 0.4 4.6 ± 1.3	0.089 ± 0.008 0.087 ± 0.020	20.2	3.43 – 12.7 22.4
2 + 1 equiv of MCPBA in acetonitrile (**9**), liquid-state EXAFS	Mn–O/N Mn-C	1.89 ± 0.02 2.90 ± 0.03	4.8 ± 0.5 4.5 ± 1.3	0.083 ± 0.008 0.067 ± 0.020	22.6	3.50 – 13.50 23.2
solid product of **2** oxidized with 2 equiv of MCPBA in acetonitrile, Solid-state EXAFS	Mn–O/N Mn–C	1.89 ± 0.02 2.89 ± 0.03	4.7 ± 0.5 4.3 ± 1.0	0.081 ± 0.008 0.063 ± 0.020	24.2	3.09 – 14.00 19.1
2 + 1 equiv of PPNO + 1 equiv of MCPBA in acetonitrile (**11**), liquid-state EXAFS	Mn–O/N Mn–C	1.89 ± 0.02 2.90 ± 0.03	3.9 ± 0.4 3.6 ± 1.3	0.084 ± 0.008 0.067 ± 0.020	21.5	3.50 – 12.90 27.6
solid product of **2** + 2 equiv of 4-PPNO oxidized with 1 equiv of MCPBA in acetonitrile, solid-state EXAFS	Mn–O/N Mn–C	1.89 ± 0.02 2.88 ± 0.03	3.9 ± 0.4 4.0 ± 1.0	0.081 ± 0.008 0.063 ± 0.020	22.1	3.10 – 12.00 23.5
[(DPPF$_{20}$)Mn^{III}Br][b] + O_3, EXAFS[29]	Mn–N_{porph} Mn–O_{ozone} Mn–O_{ozone}	4 2 2	2.00 2.09 2.49			
[(TMP)Mn^{III}Cl][c], EXAFS[14]	Mn–O Mn–N_{porph} Mn–$O_{Solv?}$	1 4 1	1.84 1.98 2.30			

[a] Absorber (A) – backscatterer (Bs) distance r, coordination number N, Debye – Waller factor σ with their calculated deviation, shift of the energy threshold ΔE_0. [b] DPP: dodecaphenyl-porphorinato manganese^{III} bromide. [c] TMP: tetramesitylporphorin.

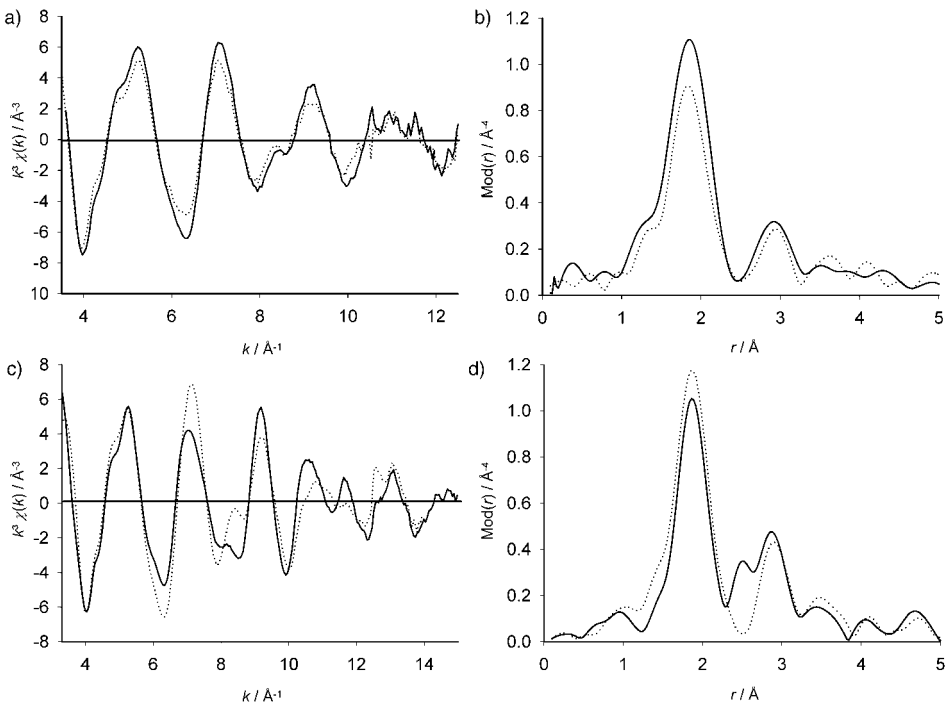

Figure 8. a,b) Comparison of the experimental $k^3\chi(k)$ functions (a) and their Fourier transforms (b) of [(salen)Mn^{III}Br]] (**2**) + MCPBA in acetonitrile (solid line, **9**), [(salen)Mn^{III}Br] (**2**) + 1 equiv of 4-PPNO + MCPBA in acetonitrile (dotted line, **11**) (Mn K-edge). c,d) Comparison of the experimental $k^3\chi(k)$ functions (c) and their Fourier transforms (d) of solid [(salen)Mn^{III}Br] (solid line, **2**) and solid [(salen)Mn^{III}Br], oxidized with MCPBA in acetonitrile (dotted line) (Mn K-edge).

and FT-EXAFS spectra of this product and pure complex **2** can be seen in Figures 8c and 8d. The structural parameters, found for this complex, are in very good agreement with those determined from the solution. Thus the complex seems to be quite stable under the condition at which the complex was produced (concentrated solution and addition of 2 equivalents of MCPBA), and no hexacoordination of the metal center was found. This result is in very good agreement with the EPR studies and mass spectral analysis of Adam et al. on a dark green solid complex,[3a] isolated from a solution of **1** + 5 equiv of NaOCl or PhIO in CH_2Cl_2. They determined the complex to be a monomeric paramagnetic (radical) manganese(IV) complex, in which an OCl or OH ligand (formed by Cl or H abstraction from CH_2Cl_2) was

© 2003 WILEY-VCH Verlag GmbH & Co. KGaA, Weinheim
0947-6539/03/0906-1356 $ 20.00+.50/0 *Chem. Eur. J.* **2003**, *9*, No. 6

coordinated to the manganese central atom. They also found a neutral Mn^{IV}=O complex as a decomposition product of the latter Mn^{IV} complexes.

Conclusion

The coordination behavior of Mn^{III} complexes upon addition of potential co-ligands, such as 4-PPNO, was determined by EXAFS and XANES studies. Such additives are usually used in salen-catalyzed epoxidations of olefins to improve epoxidation yields and enantioselectivity (stabilization of the putative oxomanganese(v) species). From the Mn K-edge and Br K-edge EXAFS spectra of the solid products of the complexes **1** and **2** with one and two equivalents of 4-PPNO, we deduced the abstraction of the halide from the manganese center with simultaneous addition of 4-PPNO. The structural parameters of the product of the reaction of **1** and **2** with two equivalents of 4-PPNO, obtained from the Mn K-edge EXAFS spectra, are consistent with an octahedral coordination around the manganese atoms (Scheme 2). The $Mn-O_{4\text{-PPNO}}$ distance was found to be 2.25 Å. From the energy shift of the 1s → 3d pre-peak in the X-ray absorption spectra, the increase of the oxidation state from Mn^{III} to Mn^{IV} is most likely accompanied by a change of the coordination from distorted tetragonal pyramidal to octahedral. These observations are in good agreement with related studies described in the literature.[30]

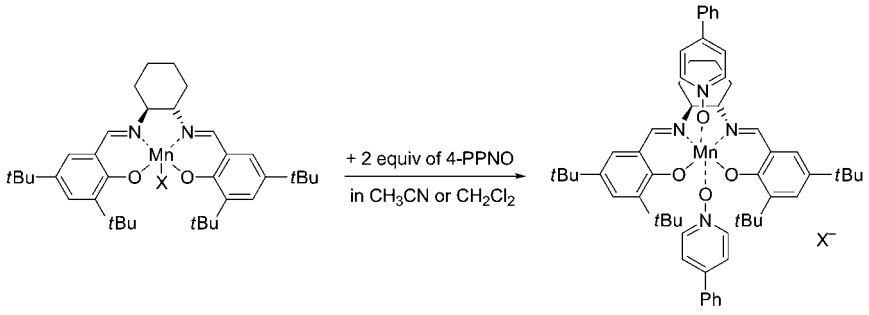

Scheme 2. Reactions of **1** and **2** with two equivalents of 4-PPNO in CH_3CN or CH_2Cl_2.

In the UV/Vis spectra of oxidized **1** and **2** (upon treatment of their solutions with MCPBA) a new broad band between 600 – 700 nm, depending on the solvent used, was observed. In the literature such absorption bands are interpreted as typical for dimeric Mn^{IV} or Mn^{IV} cation radical complexes. In very diluted samples, and in the presence of a 20-fold excess of oxidant, this green intermediate was found to be quite unstable, as indicated by the color change from green to brown and as revealed in the UV/Vis spectra by the disappearance of the new absorption band with time. In acetonitrile it was possible to monitor the reaction kinetically with UV/Vis spectroscopy. The decay reaction shows a rate law of first order with the rate constant $k_1 = 2.89 \times 10^{-3}\ s^{-1}$. However, time-dependent XANES investigations show that in very high concentrated solutions and upon addition of only one or two equivalents of MCPBA, the stability of the green complex increases significantly (stability of the green solution > 2 h). In the EXAFS spectra of the oxidized systems of the pure salen complexes **1** and **2** an additional oxygen backscatterer at ≈1.9 Å was observed. Such a distance is typical for a Mn–O single bond and was also reported for a high-valent manganese(IV) porphorinato complex.[14] The observation of a Mn–O single bond is supported by the Raman Mn–O stretching signal found in these systems at 599 cm^{-1}. An additional backscatterer, which produces a hexacoordination of the metal, was not found. From the energetic position of the 1s – 3d pre-peak in the oxidized systems one can conclude an oxidation state of the manganese atoms of +IV rather than of +V. The hypothesis that the oxidized green complex has a μ-oxo dimeric structure is wrong because no manganese backscatterers, typically found at distances of 2.6 – 2.7 Å,[19] were observed. This result is also consistent with the Raman investigations, in which no significant additional signals from a Mn–O–Mn stretching band at ≈810 cm^{-1} were observable.[7, 21] Furthermore, the presence of an oxomanganese(v) complex can be ruled out for the following three reasons: 1) no short $Mn^{V}=O_{Oxo}$ distance was found in the range of 1.5 – 1.6 Å in the EXAFS spectra, 2) the typically very high and shifted 1s – 3d pre-peak, known from the nitridomanganese(v) reference complex **3**, is absent in the oxidized systems, and 3) no Mn^{V}=O Raman signal in the range of 900 – 1000 cm^{-1} was detected. A structural proposal for the green complex, formed by the reaction of **1** and **2** with MCPBA, is shown in Scheme 3.

From those results we conclude the formation of a Mn^{IV} intermediate complex, in which an MCPBA molecule is associated with an Mn–O single bond to the manganese central atom. A radical cationic structure of this complex (explaining its high reactivity) can be assumed from the observed UV/Vis band at 640 nm. The product of the decay of the green Mn^{IV} complex in CH_2Cl_2 might be a neutral Mn^{IV}=O

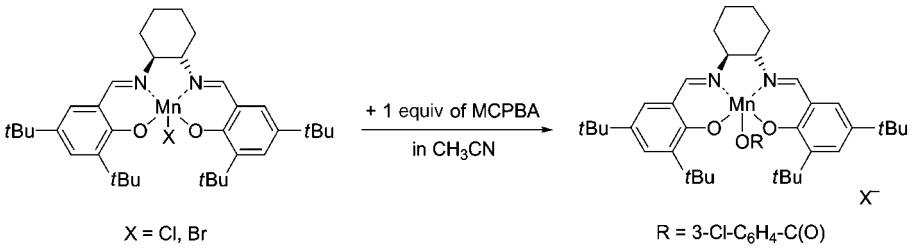

Scheme 3. Proposed reaction of **1** and **2** with one equivalent of MCPBA in CH_3CN.

 © 2003 WILEY-VCH Verlag GmbH & Co. KGaA, Weinheim 0947-6539/03/0906-1357 $ 20.00+.50/0

species, as proposed by Adam et al.,[3a] which would also explain the Raman signal at 725 cm^{-1}, observed in the solution of **1** in CH_2Cl_2 oxidized with MCPBA.

Experimental Section

Materials: [(salen)Mn^{III}] complex **1**, MCPBA, and 4-PPNO were purchased from Sigma-Aldrich Co. and used as received. Acetonitrile, toluene, and dichloromethane were spectroscopic grade (Sigma-Aldrich Co.).

Preparation of [(salen)Mn^{III}Br] (2): Bromo-(*S*,*S*)-(+)-*N*,*N*′-bis(3,5-di-*tert*-butylsalicylidene)-1,2-cyclohexanediaminomanganese(III) (**2**) was synthesized in an analogous manner to the method reported by Boucher and Farrel.[31] The product was obtained as a brown solid (2.0 g, 95%); $R_f = 0.29$ (dichloromethane:ethanol, 20:1); m.p. $>320\,^{\circ}C$; $[\alpha]_D^{20} = -1285$ ($c = 0.0184$ in chloroform); IR (KBr): $\tilde{\nu}$568, 839, 1175, 1252, 1534, 1608, 2866, 2866, 2953, 3444 cm^{-1}; MS (70 eV, EI): *m*/*z* (%): 681.3 (0.3), 679.2 (0.3) $[M]^+$, 608.3 (5), 607.3 (4), 599.3 (4), 593.3 (4), 547.4 (27), 546.4 (74), 314.2 (24), 313.2 (100), 298.2 (16), 273.3 (5), 259.0 (6), 258.2 (29), 244.2 (6), 234.2 (6), 218.2 (9), 81.2 (4), 57.2 (18), 55.2 (5); elemental analysis calcd (%) for $C_{36}H_{52}BrMnN_2O_2$ (679.7): C 63.62, H 7.71, N 4.12; found: C 63.51, H 7.80, N 4.01.

Preparation of [(salen)Mn^{V}N] (3): Nitrido-(*S*,*S*)-(+)-*N*,*N*′-bis(3,5-di-*tert*-butylsalicylidene)-1,2-cyclohexanediaminomanganese(III) (**3**) was synthesized according to the method reported by Jespen et al.[24] The product was obtained as a dark green solid (1.47 g, 65%); $R_f = 1$ (dichloromethane); m.p. $>205\,^{\circ}C$ (decomp); $[\alpha]_D^{20} = -600$ ($c = 0.000284$, CH_2Cl_2); ^1H NMR (300 MHz, $CDCl_3$, TMS): $\delta = 1.18$ (s, 2H; CH_2), 1.21 (s, 9H; CH_3), 1.21 (s, 9H; CH_3), 1.33 (s, 2H; CH_2), 1.37 (s, 9H; CH_3), 1.42 (s, 9H; CH_3), 1.94 (d, ^3J(H,H) = 6.3 Hz, 2H; CH_2), 2.85 (d, ^3J(H,H) = 11.2 Hz, 1H; CH_2), 2.60 (br s, 1H; CH_2), 2.93 (t, ^3J(H,H) = 11.2 Hz, 1H; CH), 3.36 (t, ^3J(H,H) = 9.9 Hz, 1H; CH), 7.36 (s, 1H; $CH_{ar.}$) 7.37 (s, 1H; $CH_{ar.}$), 7.39 (s, 1H; $CH_{ar.}$), 7.40 (s, 1H; $CH_{ar.}$), 7.85 (s, 1H; NCH), 7.91 ppm (s, 1H; NCH); ^{13}C NMR ($CDCl_3$, TMS): $\delta = 24.50$ (CH_2), 24.92 (CH_2), 28.79 (CH_2), 29.22 (CH_2), 30.10 (CH_2), 31.72 (CH_3), 31.71 (CH_3), 34.28 (CH_2), 34.29 (CH_2), 36.17 (CH_2), 36.22 (CH_2), 71.79 (CH), 73.63 (CH), 118.49 ($C_{ar.}$), 120.69 ($C_{ar.}$), 127.66 ($C_{ar.}$), 128.10 ($C_{ar.}$), 130.79 ($C_{ar.}$), 131.11 ($C_{ar.}$), 137.37 ($C_{ar.}$), 137.56 ($C_{ar.}$), 140.74 ($C_{ar.}$), 140.83 ($C_{ar.}$), 162.05 (CN), 162.71 (CN), 165.18 ($C_{ar.}$), 167.80 ppm ($C_{ar.}$); IR (KBr): 466, 480, 506, 1100, 1686, 1702, 1720, 1737, 1808, 2342, 2371, 3904, 3840, 3871, 3889, 3904 cm^{-1}; MS (70eV, EI): *m*/*z* (%): 613.3 (16) $[M]^+$, 546.8 (93), 313.2 (100), 258.0 (43); elemental analysis calcd (%) for $C_{36}H_{52}MnN_3O_2$ (613.7): C 70.45, H 8.54, N 6.85; found: C 70.45, H 8.50, N 6.64.

Preparation of [(salen)Mn^{III}Cl]/[(salen)Mn^{III}Br] + 4-PPNO complexes (4, 5); molar ratio of Mn complex:4-PPNO = 1:1: Complexes **1**/**2** (400 mg) were dissolved in 100 mL of CH_2Cl_2 and an equimolar amount of 4-PPNO was added. The solution was stirred for 2 hr. After evaporation of the solvent and drying of the residue under vacuum a dark brown amorphous solid (**4** from **1** and **5** from **2**) was obtained.

Preparation of [(salen)Mn^{III}Cl]/[(salen)Mn^{III}Br] + 4-PPNO complexes (6, 7); molar ratio of Mn complex:4-PPNO = 1:2: Complexes **1**/**2** (400 mg) were dissolved in CH_2Cl_2 (100 mL) and two equivalents of 4-PPNO were added. The solution was stirred for 2 h. After evaporation of the solvent and drying of the residue under vacuum, a dark brown amorphous solid (**6** from **1** and **7** from **2**) was obtained.

Preparation of oxidized [(salen)Mn^{III}Cl]/[(salen)Mn^{III}Br] samples (8, 9) for the EXAFS measurements: Complexes **1**/**2** (400 mg) were suspended in CH_3CN (4 mL) and an equimolar amount of MCPBA was added. Immediately after the addition of the oxidant the solution became clear. This dark green solution (containing **8** from **1** and **9** from **2**) was shaken vigorously for 2 min and filled into the EXAFS sample cell for liquids.

Preparation of oxidized [(salen)Mn^{III}Cl]/[(salen)Mn^{III}Br] + 4-PPNO samples (10, 11) for the EXAFS measurements: Complexes **4**/**5** (400 mg) were suspended in CH_3CN (4 mL) and an equimolar amount of MCPBA was added. Immediately after the addition of the oxidant the solution became clear. This dark green solution (containing **10** from **1** and **11** from **2**) was shaken vigorously for 2 min and filled into the EXAFS sample cell for liquids.

UV/Vis measurements: Electronic spectra were recorded on a Hewlett Packard HP 8452 diode-array spectrometer under ambient conditions (25 °C) in the wavelength range 190–800 nm with a spectral resolution of 2 nm. For the kinetic studies, solutions of **1** and **2** in CH_3CN and CH_2Cl_2 with concentrations of ≈ 0.3 mM were prepared and filled into 1 cm quartz cuvettes. The oxidant MCPBA was added in a 20-fold excess (6 mM), and the spectra were recorded every 10 s.

IR and Raman measurements: The measurements of the IR spectra were performed on a Bruker IFS 66v/S FTIR spectrometer with a DLATGS detector and a spectral resolution of 2 cm^{-1}. The samples were prepared as KBr pellets and measured under ambient conditions (512 scans). Raman spectra were recorded on a Bruker RFS 100/S Fourier Transform (FT) Raman with an air-cooled near infrared (NIR) Nd:YAG laser with a wavelength of 1064 nm and a power of 25 mW for the dark samples, such as **1** and **2**, and 150 mW for the weakly colored samples, for example **3**, 4-PPNO and the pure salen. The scattered light was collected with a high-sensitivity Ge diode (cooled with liquid nitrogen). For an average measurement, 400 scans were accumulated (spectral resolution 4 cm^{-1}). For the measurements on liquids a special Raman quartz cell was used.

XANES and EXAFS measurements: The XANES and EXAFS measurements were performed at the beamlines E4 and X1.1 (RÖMO II) at the Hamburger Synchrotronstrahlungslabor of the Deutschen Elektronen-Synchrotrons (HASYLAB at DESY, Hamburg, Germany) under ambient conditions at 25 °C. The synchrotron beam current was between 80–100 mA (positron energy 4.45 GeV). For the measurements at the Mn K-edge (6539.0 eV) a Si(111) double crystal monochromator was used at beamline E4. For the measurements at the Br K-edge a Si(311) double crystal monochromator was used at beamline X1.1. The tilt of the second monochromator crystal was set to 30% harmonic rejection. Energy resolution was estimated to be about 1.0 eV for the Mn K-edge and 4.0 eV for the Br K-edge. The spectra were collected in transmission mode with ion chambers. All ion chambers were filled with nitrogen in the case of the measurements at the Mn K-edge. The second and third ion chamber was filled with argon in the case of the measurements at the Br K-edge. Energy calibrations were performed with the corresponding metal foil in the case of manganese and with lead foil (Pb L_{III}-edge) in the case of bromine. To avoid mistakes in the Mn XANES spectra comparison due to small variations in the energy calibration between two measurements, all spectra were corrected to the theoretical edge energy of manganese foil, which was measured during each scan. The samples in the solid state were embedded in a polyethylene matrix and pressed into pellets. Liquid samples were measured in a specially designed transmission sample cell for liquids. The concentration of the solid samples was adjusted to yield an absorption jump of $\Delta\mu d \approx 1.5$.

Data evaluation started with background absorption removal from the experimental absorption spectrum by subtraction of a Victoreen-type polynomial. The background-subtracted spectrum was then convoluted with a series of increasingly broader Gauss functions and the common intersection point of the convoluted spectra was taken as energy E_0.[32, 33] To determine the smooth part of the spectrum, corrected for pre-edge absorption, a piecewise polynomial was used. It was adjusted in such a way that the low-*R* components of the resulting Fourier transform were minimal. After division of the background-subtracted spectrum by its smooth part, the photon energy was converted to photoelectron wave numbers *k*. The resulting EXAFS function was weighted with k^3. Data analysis in *k* space was performed according to the curved wave multiple scattering formalism of the program EXCURV92 with XALPHA phase and amplitude functions.[34] The mean free path of the scattered electrons was calculated from the imaginary part of the potential (VPI was set to −4.00) and an overall energy shift (ΔE_0) was assumed. The amplitude reduction factor (AFAC) was set to a value of 0.8 in the case of the Mn K-edge as well as the Br K-edge.

Acknowledgements

We wish to thank HASYLAB at DESY, Hamburg (Germany) for the kind support for the synchrotron experiments. We are also grateful to the Fonds der Chemischen Industrie and to the Deutsche Forschungsgemeinschaft (DFG) within the Graduiertenkolleg "Methods in Asymmetric Synthesis" for financial support and A. Classen for experimental contributions.

 © 2003 WILEY-VCH Verlag GmbH & Co. KGaA, Weinheim 0947-6539/03/0906-1358 $ 20.00+.50/0 *Chem. Eur. J.* **2003**, *9*, No. 6

[1] a) R. A. Sheldon, J. K. Kochi, *Metal-Catalyzed Oxidations of Organic Compounds*, Academic Press, New York, **1981**; b) A. S. Rao in *Comprehensive Organic Synthesis*, *Vol. 7* (Eds.: B. M. Trost, I. Fleming), Pergamon, Oxford, **1991**, pp. 357; c) K. Muñiz-Fernández, C. Bolm, in *Transition Metals for Organic Synthesis*, *Vol. 2* (Eds.: M. Beller, C. Bolm), VCH-Wiley, Weinheim, **1998**, pp. 271; d) K. A. Jørgensen, *Chem. Rev.* **1989**, *89*, 431; e) V. Schurig, F. Betschinger, *Chem. Rev.* **1992**, *92*, 873; f) P. Besse, H. Veschambre, *Tetrahedron* **1994**, *50*, 8885; g) S. Pedragosa-Moreau, A. Archelas, R. Furstoss, *Bull. Soc. Chim. Fr.* **1995**, *132*, 769; h) A. Archelas, R. Furstoss, *Top. Curr. Chem*. **1999**, *200*, 159.

[2] a) E. N. Jacobsen, in *Catalytic Asymmetric Synthesis* (Ed.: I. Ojima), VCH, New York, **1993**, pp. 159; b) E. N. Jacobsen, *Acc. Chem. Res.* **2000**, *33*, 421; c) T. Katsuki, in *Catalytic Asymmetric Synthesis*, 2nd ed. (Ed.: I. Ojima), Wiley-VCH, New York, **2000**, pp. 287; d) T. Katsuki, in *Comprehensive Asymmetric Catalysis*, *Vol. 2* (Eds.: E. N. Jacobsen, A. Pfaltz, H. Yamamoto), Springer, Berlin, **1999**, pp. 621; e) T. Katsuki, *Coord. Chem. Rev.* **1995**, *140*, 189; f) T. Katsuki, *J. Mol. Catal. A* **1996**, *113*, 87; g) Y. N. Ito, T. Katsuki, *Bull. Chem. Soc. Jpn*. **1999**, *72*, 603; h) T. Katsuki, *Adv. Synth. Catal.* **2002**, *344*, 131; i) C. T. Dalton, K. M. Ryan, V. M. Wall, C. Bousquet, D. G. Gilheany, *Top. Catal*. **1998**, *5*, 75; j) T. Flessner, S. Doye, *J. Prakt. Chem*. **1999**, *341*, 436.

[3] a) W. Adam, C. Mock-Knoblauch, C. R. Saha-Möller, M. Herderich, *J. Am. Chem. Soc.* **2000**, *122*, 9685; b) T. Linker, *Angew. Chem*. **1997**, *109*, 2150; *Angew. Chem. Int. Ed. Engl.* **1997**, *36*, 2060; c) K. A. Jørgensen in *Transition Metals for Organic Synthesis*, *Vol. 2* (Eds.: M. Beller, C. Bolm), VCH-Wiley, Weinheim, **1998**, pp. 157; d) C. Linde, B. Åkermark, P.-O. Norrby, M. Svensson, *J. Am. Chem. Soc.* **1999**, *121*, 5083; e) T. Strassner, K. N. Houk, *Org. Lett.* **1999**, *1*, 419; f) L. Cavallo, H. Jacobsen, *Angew. Chem.* **2000**, *112*, 602; *Angew. Chem. Int. Ed. Engl.* **2000**, *39*, 589; g) H. Jacobsen, L. Cavallo, *Chem. Eur. J.* **2001**, *7*, 800; h) C. Linde, N. Koliai, P.-O. Norrby, B. Åkermark, *Chem. Eur. J.* **2002**, *8*, 2568, and references therein.

[4] a) N. S. Finney, P. J. Pospisil, M. L. Güler, T. Ishida, E. N. Jacobsen, *Angew. Chem*. **1997**, *109*, 1798; *Angew. Chem. Int. Ed. Engl.* **1997**, *36*, 1720; b) M. Palucki, N. S. Finney, P. J. Pospisil, M. L. Güler, T. Ishida, E. N. Jacobsen, *J. Am. Chem. Soc*. **1998**, *120*, 948.

[5] a) C. Linde, M. Arnold, P.-O. Norrby, B. Åkermark, *Angew. Chem*. **1997**, *109*, 1802; *Angew. Chem. Int. Ed. Engl.* **1997**, *36*, 1723; b) T. Hamada, T. Fukuda, H. Imanishi, T. Katsuki, *Tetrahedron* **1996**, *52*, 515.

[6] For the general importance of the concept of spin-state crossings in metal–oxo systems, see: a) S. Shaik, M. Filatov, D. Schröder, H. Schwarz, *Chem. Eur. J.* **1998**, *4*, 193; b) D. Schröder, S. Shaik, H. Schwarz, *Acc. Chem. Res.* **2000**, *33*, 139; c) D. A. Plattner, *Angew. Chem*. **1999**, *111*, 86; *Angew. Chem. Int. Ed. Engl.* **1999**, *38*, 82.

[7] J. A. Smegal, B. C. Schardt, C. L. Hill, *J. Am. Chem. Soc.* **1983**, *105*, 3510.

[8] a) D. Feichtinger, D. Plattner, *Angew. Chem.* **1997**, *109*, 1796; *Angew. Chem. Int. Ed. Engl.* **1997**, *36*, 1718; b) D. Feichtinger, D. Plattner, *J. Chem. Soc. Perkin Trans. 2* **2000**, 1023; c) D. Feichtinger, D. Plattner, *Chem. Eur. J.* **2001**, *7*, 591; d) J. El-Bahraoui, O. Wiest, D. Feichtinger, D. Plattner, *Angew. Chem.* **2001**, *113*, 2131; *Angew. Chem. Int. Ed. Engl.* **2001**, *40*, 2073.

[9] a) R. Irie, Y. Ito, T. Katsuki, *Synlett* **1991**, 265; b) K. Miura, T. Katsuki, *Synlett* **1991**, 783; c) see also: D. J. Highes, G. B. Smith, J. Liu, G. C. Dezeny, C. H. Senanayake, R. D. Larsen, T. R. Verhoeven, P. J. Reider, *J. Org. Chem*. **1997**, *62*, 2222.

[10] a) H. Bertagnolli, T. S. Ertel, *Angew. Chem.* **1994**, *106*, 15; *Angew. Chem. Int. Ed. Engl*. **1994**, *33*, 45; b) G. Kickelbick, U. Reinöhl, T. S. Ertel, H. Bertagnolli, K. Matyajaszewski in *The Copper Catalyst in Atom Transfer Radical Polymerizations: Structural Observations Controlled/Living Radical Polymerization* (Ed.: K. Matyaszewski), American Chemical Society, Washington, DC, **2000**, pp. 211; c) E. Lindner, F. Auer, A. Baumann, P. Wegner, H. A. Mayer, H. Bertagnolli, U. Reinöhl, T. S. Ertel, A. Weber, *J. Mol. Catal. A* **2000**, *157*, 97; d) G. Kickelbick, U. Reinöhl, T. S. Ertel, A. Weber, H. Bertagnolli, K. Matyjaszewski, *Inorg. Chem*. **2001**, *40*, 6.

[11] M. T. Rispens, A. Meetsma, B. L. Feringa, *Recl. Trav. Chim. Pays-Bas* **1994**, *113*, 413.

[12] A. Biaconi in *EXAFS and Near Edge Structure II* (Eds.: K. O. Hodgson, B. Hedman, J. E. Penner-Hahn) Springer Proceedings in Physics **1984**, *2*, 167.

[13] F. Wong, F. W. Lytle, R. P. Messmer, D. H. Maylotte, *Phys. Rev.* **1984**, *B 30*, 5596.

[14] O. Bortolini, M. Ricci, B. Meunier, P. Friant, I. Ascone, J. Goulon, *New J. Chem*. **1986**, *10*, 39.

[15] TMP = chloro-(5,10,15,20-*meso*-tetramesitylporphorinato)manganese(III); TPP = dimethoxy(5,10,15,20-tetraphenylporphorinato)manganese(IV); salpn = *N*,*N*′-bis(salicylidene)-1,3-diaminopropane; VOPBD = vanadyl bis(1-phenyl-1,3-butane) dionate; PNO = pyridine *N*-oxide.

[16] K. Srinisvasan, P. Michaud, J. K. Kochi, *J. Am. Chem. Soc.* **1986**, *108*, 2309.

[17] M. J. Camenzind, F. J. Hollander, C. L. Hill, *Inorg. Chem*. **1982**, *21*, 4301.

[18] J. T. Groves, J. Lee, S. S. Marla, *J. Am. Chem. Soc.* **1997**, *119*, 6269.

[19] M. J. Baldwin, N. A. Law, T. L. Stemmler, J. W. Kampf, J. E. Penner-Hahn, V. L. Pecoraro, *Inorg. Chem.* **1999**, *38*, 4801.

[20] S. S. Mitra, S. Nudelman, *Far-Infrared Properties of Solids*, Proceedings of a NATO Advanced Study Institute (1968), Delft, Netherlands, Plenum Press, **1970**, pp. 488.

[21] B. C. Schardt, F. J. Hollander, G. L. Hill, *J. Am. Chem. Soc.* **1982**, *104*, 3964.

[22] E. G. Samsel, K. Srinivasan, J. K. Kochi, *J. Am. Chem. Soc.* **1985**, *107*, 7606.

[23] a) J. Du Bois, J. Hong, E. M. Carreira, M. W. Day, *J. Am. Chem. Soc.* **1996**, *118*, 915; b) J. W. Buchler, C. Dreher, K.-L. Lay, Y. J. A. Lee, W. R. Scheidt, *Inorg. Chem.* **1983**, *22*, 888; c) J. Weidlein, U. Müller, K. Dehnicke, *Schwingungsfrequenzen II*, Georg Thieme Verlag, Stuttgart, **1986**.

[24] A. S. Jepsen, M. Roberson, R. G. Hazell, K. A. Jørgensen, *Chem. Commun*. **1998**, 1599.

[25] a) R. J. Nick, G. B. Ray, K. M. Fish, T. G. Spirpo, J. T. Groves, *J. Am. Chem. Soc.* **1991**, *113*, 1838; b) R. S. Czernuszewicz, Y. O. Su, M. K. Stern, K. A. Macor, D. Kim, J. T. Groves, T. G. Spiro, *J. Am. Chem. Soc*. **1988**, *110*, 4158; c) J. T. Groves, M. K. Stern, *J. Am. Chem. Soc.* **1988**, *110*, 8628.

[26] a) D. C. Konigsberger, R. Prins, *X-Ray Absorption: Principles*, *Applications*, *Techniques of EXAFS*, *SEXAFS and XANES*, Wiley, New York, **1988**; b) B. K. Teo, *EXAFS: Basic Principles and Data Analysis*, Springer, Berlin, **1986**; c) J. Stöhr, *NEXAFS Spectroscopy*, Springer, Berlin, **1996**.

[27] F. W. Kutzler, C. R. Natoli, D. K. Misemer, S. Doniach, K. O. Hodgson, *J. Chem. Phys.* **1980**, *73*, 3274.

[28] P. J. Pospisil, D. H. Carsten, E. N. Jacobsen, *Chem. Eur. J.* **1996**, *2*, 974.

[29] V. Gotte, J. Goulon, C. Goulon-Ginet, A. Rogalev, C. R. Natoli, K. Perié, J. M. Barbe, R. Guilard, *J. Phys. Chem. B* **2000**, *104*, 1927.

[30] K. A. Campbell, M. R. Lashley, J. K. Wyatt, M. H. Nantz, R. D. Britt, *J. Am. Chem. Soc.* **2001**, *123*, 5710.

[31] L. J. Boucher, M. O. Farrel, *J. Inorg. Nucl. Chem.* **1973**, 35, 3731.

[32] T. S. Ertel, H. Bertagnolli, S. Hückmann, U. Kolb, D. Peter, *Appl. Spectrosc.* **1992**, *46*, 690.

[33] M. Newville, P. Livins, Y. Yakoby, J. J. Rehr, E. A. Stern, *Phys. Rev. B* **1993**, *47*, 14126.

[34] S. J. Gurman, N. Binsted, I. Ross, *J. Phys. C* **1986**, *C 19*, 1845.

Received: August 6, 2002
Revised: October 28, 2002 [F4321]

 © 2003 WILEY-VCH Verlag GmbH & Co. KGaA, Weinheim 0947-6539/03/0906-1359 $ 20.00+.50/0